DOI: 10.35840/2631-5092/4520

VIBGYOR ePress

International Journal of
Optic and Photonic Engineering

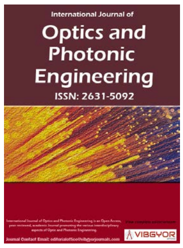

ISSN: 2631-5092

Dynamical Characteristics of External Cavity Quantum Cascade Lasers

***Abdelouahab Hamadou*[1,2*]**

[1]*Département de Génie Civil, Faculté des Sciences et de la Technologie, Université Mohamed El Bachir El Ibrahimi, Bordj Bou Arreridj 34000, Algeria*

[2]*Laboratoire d'étude des Surfaces et Interfaces des Matériaux Solides (LESIMS), Université Ferhat Abbas Sétif1, 19000, Algeria*

Abstract

In this paper, we calculate the dynamical characteristics such as delay time, rise time, and time to steady state establishment, of a mid infrared quantum cascade laser coupled to external cavity. The approach is based on the three-level rate equations including the dependence of the loss on external cavity parameters. We find in particular that the threshold current of external cavity is strongly influenced by the external reflectivity and external cavity length. In addition, the equations that allow for the determination of the dynamical characteristics are derived within the premises of our model in the general case. The effects of the external cavity parameters on dynamical characteristics are also explored.

Keywords

Quantum cascade laser, External cavity, Delay time, Rise time, Time to steady state establishment

Introduction

After the first demonstration of the quantum cascade (QC) laser by Faist in 1994 [1], external cavity (EC) QC laser was demonstrated for the first time by Luo in 2001 [2]. In recent years, different works on EC-QC lasers were published because of their useful characteristics such as spectral tuning rang and single mode operation [3-14].

It is well known that EC strongly affects the losses, photon lifetime and threshold current of QC laser, and thus influence the turn on delay time where it decreases with increasing external reflectivity [10,11,14,15]. Equally as important for the EC-QC laser operation is the delay time, rise time, and time to steady state establishment (TSSE). Therefore, studies of EC-QC laser are important for potential applications in intersubband photonics field. In this paper, we calculate the delay time (t_d^{EC}), the rise time (Δt_{rise}^{EC}), and the TSSE (t_{ss}^{EC}) in terms of current injection, threshold current, scattering times, and photon lifetime for the external cavity, using a rate equations model. It is an extension of the

***Corresponding author:** *Abdelouahab Hamadou, Département de Génie Civil, Faculté des Sciences et de la Technologie, Université Mohamed El Bachir El Ibrahimi, Bordj Bou Arreridj 34000, Algeria; Laboratoire d'étude des Surfaces et Interfaces des Matériaux Solides (LESIMS), Université Ferhat Abbas Sétif1 19000, Algeria, Tel: +213776937575*

Accepted: December 10, 2019; **Published:** December 12, 2019

Hamadou. Int J Opt Photonic Eng 2019, 4:020

ISSN 2631-5092

Citation: Hamadou A (2019) Dynamical Characteristics of External Cavity Quantum Cascade Lasers. Int J Opt Photonic Eng 4:020

previous work reported in Ref [15].

The Model

Figure 1 shows the schematic illustration of a cavity model for the QC laser with external cavity that we treat here. The output power from a Fabry-Perot QC laser cavity (length L and reflectivities R_1 and R_2) is reflected by an external mirror of reflectance R_{ext}, which is located at a distance L_{ext} from the front facet of the QC laser. The dynamics of EC-QC laser can be described by a three-level model. The upper and lower states will be taken as levels 3 and 2, respectively, while the ground state used to empty the lower state through longitudinal optical phonon (LO) emission will be called level 1.

The system of rate equations for electron numbers N_1, N_2 and N_3 in levels 1, 2 and 3, and the photon numbers S^{FP} and S^{EC} in the FP and in the EC is used to model the dynamic behavior of EC-QC laser in this work [15].

$$\frac{dN_3}{dt} = \frac{I_{inj}}{e} - \frac{N_3}{\tau_3} - \left(G^{FP}S^{FP} + G^{EC}S^{EC}\right)(N_3 - N_2), \tag{1a}$$

$$\frac{dN_2}{dt} = \frac{N_3}{\tau_{32}} - \frac{N_2}{\tau_{21}} + \left(G^{FP}S^{FP} + G^{EC}S^{EC}\right)(N_3 - N_2), \tag{1b}$$

$$\frac{dN_1}{dt} = \frac{N_3}{\tau_{31}} + \frac{N_2}{\tau_{21}} - \frac{N_1}{\tau_{out}}, \tag{1c}$$

$$\frac{dS^{FP}}{dt} = N_p G^{FP}(N_3 - N_2)S^{FP} + N_p \beta \frac{N_3}{\tau_{sp}} - \frac{S^{FP}}{\tau_p^{FP}}, \tag{1d}$$

$$\frac{dS^{EC}}{dt} = \frac{1}{\rho_{cav}}\left(N_p G^{EC}(N_3 - N_2)S^{EC} + N_p \beta \frac{N_3}{\tau_{sp}} - \frac{S^{EC}}{\tau_p^{EC}}\right). \tag{1e}$$

Where I_{inj} is the injected current, e is the electron charge, τ_{32}, τ_{31}, and τ_{21} are the nonradiative scattering times between the corresponding levels due to LO-phonon emission, τ_{sp} is the radiative spontaneous relaxation time between levels 3 and 2, τ_3 is the lifetime of the upper level and defined as $\tau_3 = 1/(1/\tau_{32} + 1/\tau_{31})$, τ_{out} is the electron escape time between two adjacent stages [16], β defines the fraction of the spontaneous emission light emitted in the lasing mode [17], N_p is the number of stages, $\rho_{cav} = 1 + L_{ext}/(n_{eff}L)$ is the ratio of optical path lengths of the FP and the external cavity [18] where n_{eff} is the effective refractive index of FP active region, and G^{EC} and G^{EC} are the gain coefficients per period in the FP and in the external cavity respectively. The latter is defined through [14].

$$G^{EC} = G^{FP} \frac{\gamma_{32}^2}{\left(h\nu^{EC} - h\nu^{FP}\right)^2 + \gamma_{32}^2}, \tag{2}$$

Where $2\gamma_{32}$ stands for the full width at half maximum of the electroluminescence spectrum between levels 3 and 2, h is the Planck constant, and ν is the lasing frequency.

The parameters τ_p^{FP} and τ_p^{EC} in Eqs.(1d-e) are respectively the lifetimes of the photons in the FP active region and in the EC [15] and given as function of waveguide loss of the cavity α_w and the mirrors losses by

$$\tau_p^{FP} = \frac{2L}{c'} \frac{1}{\left(2L\alpha_w - \ln\left(R_1 R_2\right)\right)}, \tag{3a}$$

$$^{EC} = \frac{2}{'} \frac{1}{\left(2L \quad _w \quad \ln\left(R\, R_{eff}\right)\right)}, \tag{3b}$$

Where R_{eff} is the effective reflectivity of the equivalent EC-QC laser and can be written as [19].

$$R_{eff} = \frac{R_2 + R_{ext} + 2\sqrt{R_2 R_{ext}}\cos(\omega\tau)}{1 + R_2 R_{ext} + 2\sqrt{R_2 R_{ext}}\cos(\omega\tau)}, \tag{4}$$

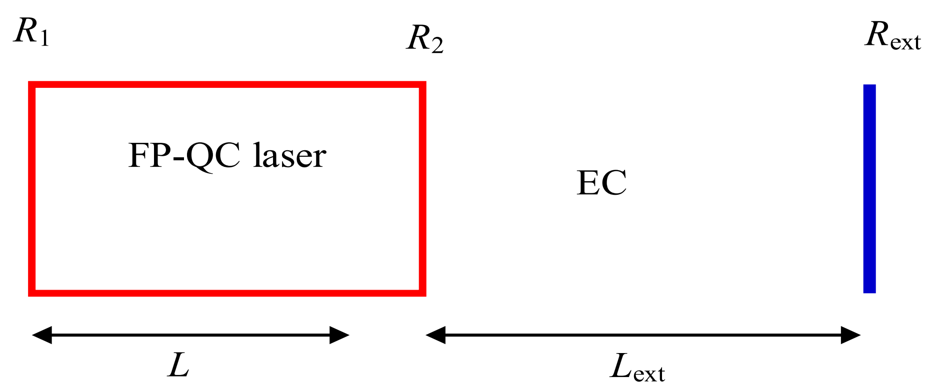

Figure 1: Schematic illustration of a cavity model for a QC laser with external cavity.

Where ω is the laser angular frequency, $\tau = 2L_{ext}/c$ is the round-trip time of light in the external cavity and where c is the speed of light in vacuum.

In Eq. (3) we have assumed for simplicity that the waveguide loss of the EC mode is the same as that for the FP mode i.e., $\alpha_w^{EC} = \alpha_w^{FP} = \alpha_w$.

Under steady state conditions, the electron numbers in the upper and lower laser levels obey the following relations

$$N_3 = \frac{\frac{I_{inj}}{e}\tau_3\left(1+\frac{\tau_{21}}{\tau_3(1+\frac{\tau_{21}}{\tau_{31}})}\left(\frac{S^{FP}}{S^{FP}_{sat}}+\frac{S^{EC}}{S^{EC}_{sat}}\right)\right)}{1+\frac{S^{FP}}{S^{FP}_{sat}}+\frac{S^{EC}}{S^{EC}_{sat}}}, \quad (5a)$$

$$N_2 = \frac{\frac{I_{inj}}{e}\tau_3\left(\frac{\tau_{21}}{\tau_{32}}+\frac{\tau_{21}}{\tau_3(1+\frac{\tau_{21}}{\tau_{31}})}\left(\frac{S^{FP}}{S^{FP}_{sat}}+\frac{S^{EC}}{S^{EC}_{sat}}\right)\right)}{1+\frac{S^{FP}}{S^{FP}_{sat}}+\frac{S^{EC}}{S^{EC}_{sat}}}, \quad (5b)$$

Where we introduced the photon saturation number for both modes S^i_{sat} given by

$$S^i_{sat} = \frac{1}{\tau_3(1+\frac{\tau_{21}}{\tau_{31}})G^i}, \quad (6)$$

Where the superscript *i* refer to the FP or EC mode.

The population inversion ΔN between the upper and lower levels as a function of the FP and EC photon numbers can be then written by using Eqs. (5a-b) as

$$\Delta N = \frac{\frac{I_{inj}}{e}\tau_3(1-\frac{\tau_{21}}{\tau_{32}})}{1+\frac{S^{FP}}{S^{FP}_{sat}}+\frac{S^{EC}}{S^{EC}_{sat}}}. \quad (7)$$

Combining Eqs.(5a), (6), and (7) with Eq.(1e), the following expression is then obtained for ^{EC}:

$$S^{EC} \approx \left(\frac{I_{inj}}{I^{EC}_{th}}-1-\frac{S^{FP}}{S^{FP}_{sat}}+\frac{1}{(1+\frac{\tau_{21}}{\tau_{31}})}\frac{\beta}{\tau_{sp}}\frac{\tau_{21}}{\eta_r}\frac{I_{inj}}{I^{EC}_{th}}\right)S^{EC}_{sat}. \quad (8)$$

Where I^{EC}_{th} is the threshold current under the effect of external cavity while the parameter $\eta_r = \left(1-\tau_{21}/\tau_{32}\right)/\left(1+\tau_{21}/\tau_{31}\right)$ is the radiative efficiency.

At threshold condition, the rate of photon production inside the external cavity is equal to the rate of photon loss, *i.e.*, $N_p G^{EC}\Delta N^{EC}_{th} = 1/\tau^{EC}_p$, the threshold population inversion is given by

$$\Delta N^{EC}_{th} = \frac{1}{N_p\tau^{EC}_p G^{EC}}. \quad (9)$$

The threshold current I^{EC}_{th} is obtained from Eq.(7) by setting S^{FP} and S^{EC} to zero and making I^{EC}_{th} replace I_{inj}. With the help of Eq.(9) we get after easy algebra for I^{EC}_{th} the following expression

$$I^{EC}_{th} = \frac{e}{N_p G^{EC}\tau_3(1-\frac{\tau_{21}}{\tau_{32}})\tau^{EC}_p}. \quad (10)$$

In the some way, the threshold current for the FP can be defined as

$$I^{FP}_{th} = \frac{e}{N_p G^{FP}\tau_3(1-\frac{\tau_{21}}{\tau_{32}})\tau^{FP}_p}. \quad (11)$$

Next using the theory developed above we estimate numerically I^{FP}_{th}, τ^{FP}_p, G^{EC}, and S^{EC}_{sat} using the following experimental QC laser parameters as reported in Refs. [14-16]: L = 1.5 mm, R_1 = 0.8, R_2 = 0.01, α_w = 14 cm^{-1}, N_p = 48, β = 1 × 10^{-3}, n_{eff} = 3.27, τ_{32} = 2.4 ps, τ_{31} = 3 ps, τ_{21} = 0.4 ps, τ_{out} = 1 ps, τ_{sp} =140 ns, λ = 8 µm, $G^{FP} = 2\times10^3$ s^{-1}, $\omega^{FP} \approx \omega^{EC}$. Our results are as follows: $\tau^{FP}_p = 3.6$ ps, I^{FP}_{th} = 0.4 A, $G^{EC} = 2\times10^3$, and $S^{EC}_{sat} = 3.17\times10^8$.

Figure 2 shows the variation of the threshold current I^{EC}_{th} with external cavity length L_{ext} for an external cavity reflectivity $R_{ext} = 90\%$. As seen from this figure, the threshold current varies periodically with the external cavity length. The period of undulation is about 4 cm. The low threshold current occurs at the L_{ext} of around 4, 8 or 12 cm that produced minimum threshold current of 198.7 mA. In Figure 3, the threshold current I^{EC}_{th} is plotted versus external cavity reflectivity R_{ext} for an external cavity length $L_{ext} = 8$ cm. We can easily see that the threshold current is a decreasing function of external cavity reflectivity. This is attributed to the increases of photon lifetime in the EC with R_{ext}. We show also that by increasing

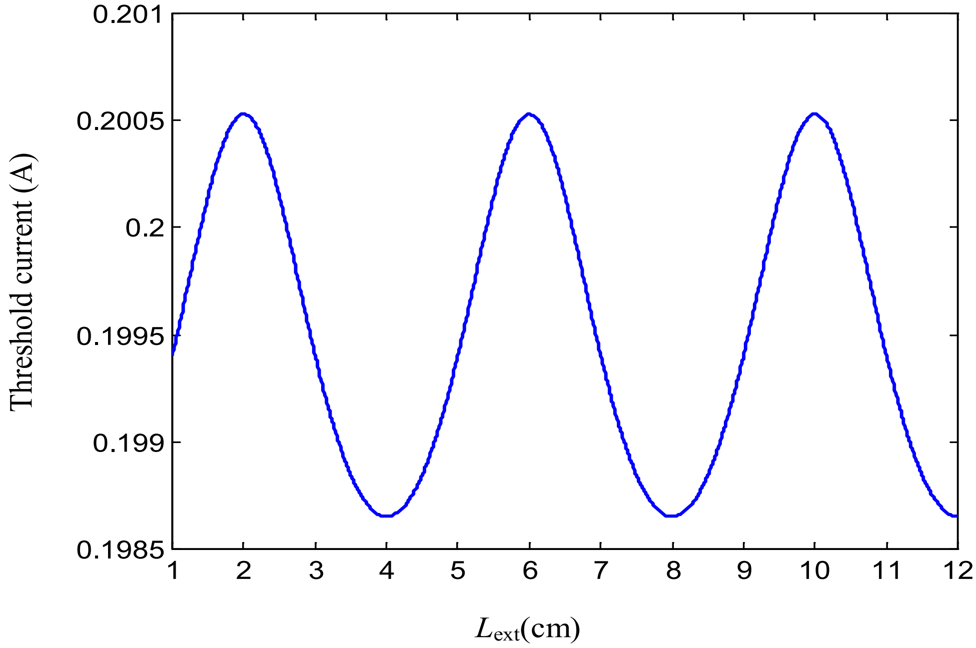

Figure 2: Effect of external cavity length (L_{ext}) on threshold current I_{th}^{EC} . The external cavity reflectivity is $R_{ext} = 90\%$.

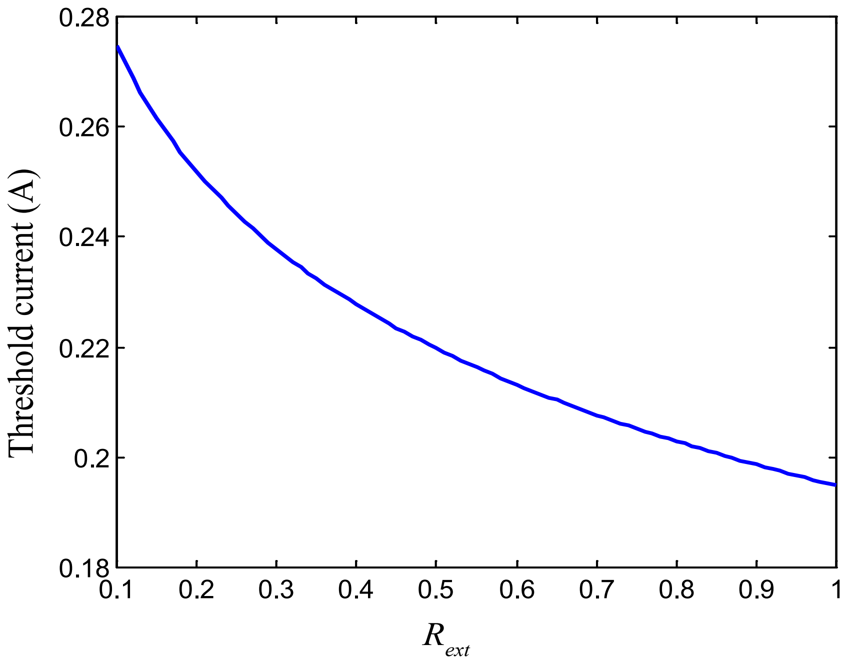

Figure 3: Effect of external cavity reflectivity (R_{ext}) on threshold current I_{th}^{EC} . The external cavity length is $L_{ext} = 8$ cm.

the external cavity reflectivity from 10% to 100%, the threshold current decreased from 0.275 A to 0.195 A.

Dynamical Analysis

Numerical analysis

The temporal evolution of the photon numbers S^{FP} and S^{EC} is analyzed by numerically solving the system of nonlinear differential equations given in Eq.(1) using the fourth-order Runge-Kutta method. The results are all obtained for an external cavity length $L_{ext} = 8$ cm and an external cavity reflectivity $R_{ext} = 90\%$. The following initial conditions for electron numbers and photon numbers are: $N_1(0) = N_2(0) = N_3(0) = 0$ and $S^{FP}(0) = S^{EC}(0) = 0$. In addition, the injection currents are assumed corresponding to the constant value of $I_{th}^{10\%}$ (i.e., $I_{inj} = bI_{th}^{10\%}$, where $I_{th}^{10\%} = 0.275$ A is the threshold current at $R_{ext} = 10\%$).

The temporal evolution of the photon numbers S^{FP} and S^{EC} of the two modes for an injection current $I_{inj} = 2I_{th}^{10\%}$ is displayed in Figure 4. Also shown on the same figure are the three dynamical characteristics times: (*i*) A delay time interval (t_d^{EC}) where the number of photons in the EC reaches 10% of its stationary value. In the conditions of Figure 4, this extends from the time origin given by the bias current to about 1.8 ns, (*ii*) A time taken for S^{EC} to rise from 10% to 90% of its stationary value. In Figure 4, it extends from 1.8 ns to about 2.4 ns. This period is called the rise time (Δt_{rise}^{EC}), (*iii*) A long time interval where the laser reaches its stationary regime. In the conditions of Figure 4, this goes at about 3ns after the start of current injection. This period is called the TSSE (t_{ss}^{EC}). The results of Figure 4 show that the FP number of photons reaches its maximum and stabilizes within less then 0.5 ns, followed by a delay time for the EC number of photons to buildup and to reach its maximum, accompanied by the simultaneous decay of the FP number of photons. This delay time is of around of 1.8 ns.

Derivation of the dynamical characteristics of EC-QC laser

In this section, we first derive approximate analytical time-dependent solutions of the rate equations above external cavity QC laser threshold and we present our results to derive the expressions that allow for the determination of the dynamical characteristics of external cavity such as t_d^{EC}, Δt_{rise}^{EC}, and t_{ss}^{EC}.

The system of EC-QC laser rate equations are difficult to solve analytically. The derivation of the approximate solutions of the system can be substantiated analytically by employing adiabatic

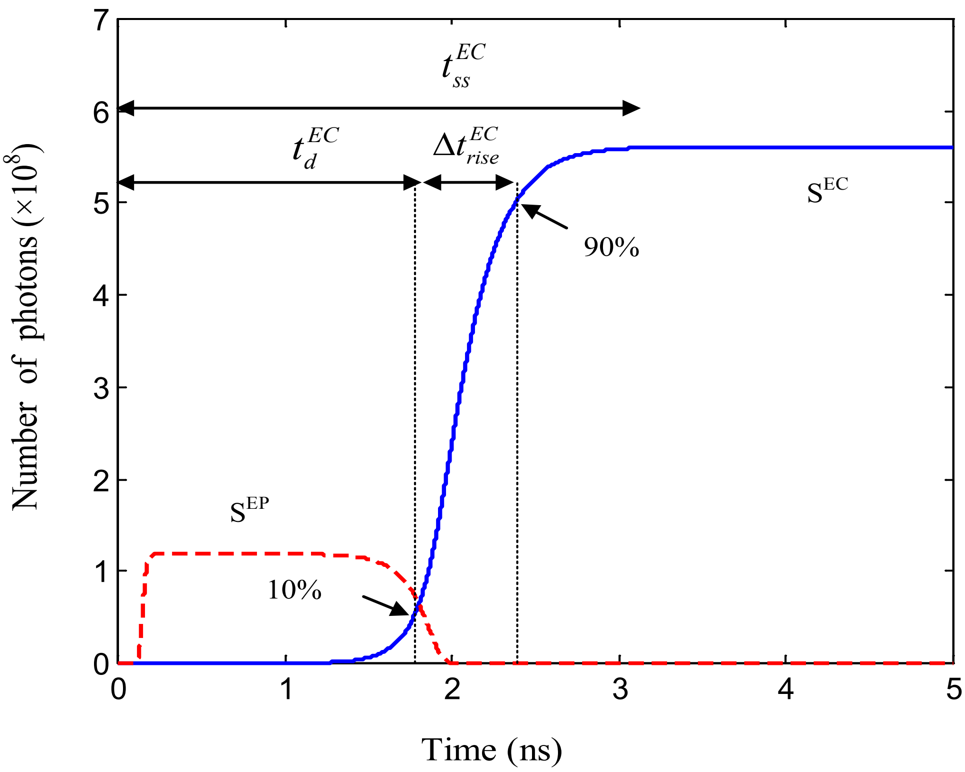

Figure 4: Time evolution of S^{FP} and S^{EC} for an current injection $I_{inj} = 2I_{th}^{10\%}$. The external cavity length is $L_{ext} = 8$ cm and the external reflectivity $R_{ext} = 90\%$. We note three distinct times: delay time (t_d^{EC}), rise time (Δt_{rise}^{EC}), and TSSE (t_{ss}^{EC}).

elimination technique. This analysis is described in [20].

According to the results obtained in [20], we can make the time-dependent of photon numbers $S^{FP}(t)$ and $S^{EC}(t)$ replace S^{FP} and S^{EC} in the Eqs. (5a-b) and add in these the temporal expressions that describe the overshoot behaviour of number of electrons in the upper and lower laser levels, we obtain for $N_3(t)$ and $N_2(t)$ the following expressions

$$N_3(t) = \frac{I_{inj}}{e}\tau_3 \frac{\left(1+\frac{\tau_{21}}{\tau_3(1+\frac{\tau_{21}}{\tau_{31}})}\left(\frac{S^{FP}(t)}{S_{sat}^{FP}}+\frac{S^{EC}(t)}{S_{sat}^{EC}}\right)\right)}{1+\frac{S^{FP}(t)}{S_{sat}^{FP}}+\frac{S^{EC}(t)}{S_{sat}^{EC}}}\left(1-e^{-\frac{t}{\tau_3}}\right), \quad (12a)$$

$$N_2(t) = \frac{I_{inj}}{e}\tau_3 \frac{\left(\frac{\tau_{21}}{\tau_{32}}+\frac{\tau_{21}}{\tau_3(1+\frac{\tau_{21}}{\tau_{31}})}\left(\frac{S^{FP}(t)}{S_{sat}^{FP}}+\frac{S^{EC}(t)}{S_{sat}^{EC}}\right)\right)}{1+\frac{S^{FP}(t)}{S_{sat}^{FP}}+\frac{S^{EC}(t)}{S_{sat}^{EC}}}\left(1-\frac{e^{-\frac{t}{\tau_{21}}}}{1-\frac{\tau_3}{\tau_{21}}}+\frac{e^{-\frac{t}{\tau_3}}}{\frac{\tau_{21}}{\tau_3}-1}\right). \quad (12b)$$

From Eqs.(12a-b), we deduce the intersubband time-dependent population inversion $\Delta N(t)$ under the effect of external cavity as

$$\Delta N(t) = \frac{I_{inj}}{e}\left(\frac{\xi_0+\left(\xi_1+\xi_2(\frac{S^{FP}(t)}{S_{sat}^{FP}}+\frac{S^{EC}(t)}{S_{sat}^{EC}})\right)e^{-\frac{t}{\tau_{21}}}-\left(\xi_3+\xi_4(\frac{S^{FP}(t)}{S_{sat}^{FP}}+\frac{S^{EC}(t)}{S_{sat}^{EC}})\right)e^{-\frac{t}{\tau_3}}}{1+\frac{S^{FP}(t)}{S_{sat}^{FP}}+\frac{S^{EC}(t)}{S_{sat}^{EC}}}\right), \quad (13)$$

Where

$$\xi_0 = \tau_3\left(1-\frac{\tau_{21}}{\tau_{32}}\right),$$

$$\xi_1 = \frac{\tau_{21}^2}{\tau_{32}}\frac{1}{\left(\frac{\tau_{21}}{\tau_3}-1\right)},$$

$$\xi_2 = \frac{\tau_{21}^2}{\tau_3}\frac{1}{\left(1+\frac{\tau_{21}}{\tau_{31}}\right)\left(\frac{\tau_{21}}{\tau_3}-1\right)},$$

$$\xi_3 = \tau_3+\frac{\tau_3\tau_{21}}{\tau_{32}}\frac{1}{\left(\frac{\tau_{21}}{\tau_3}-1\right)},$$

$$\xi_4 = \xi_2 \quad (14)$$

The functions $\exp(-t/\tau_3)$ and $\exp(-t/\tau_{21})$ in Eq.(13) vanish quickly and these terms can be omitted. Thus, we rewrite Eq.(13) in the form

$$\Delta N(t) = \frac{\frac{I_{inj}}{e}\tau_3\left(1-\frac{\tau_{21}}{\tau_{32}}\right)}{1+\frac{S^{FP}(t)}{S_{sat}^{FP}}+\frac{S^{EC}(t)}{S_{sat}^{EC}}}. \quad (15)$$

The expressions for the number of electrons in the upper level $N_3(t)$ and the population inversion $\Delta N(t)$ variables are now substituted back into the photon number Eq.(1e) to give the following nonlinear equation, expressed with the help of Eq.(6) as

$$\frac{dS^{EC}(t)}{dt}\tau_p^{EC}\rho_{cav}\frac{dS^{EC}(t)}{dt} = \frac{\frac{N_p\beta\tau_3\tau_p^{EC}I_{inj}}{\tau_{sp}e}\left(1+\frac{\tau_{21}}{\tau_3(1+\frac{\tau_{21}}{\tau_{31}})}\frac{S^{FP}(t)}{S_{sat}^{FP}}\right)+\left(\frac{I_{inj}}{I_{th}^{EC}}-1-\frac{S^{FP}(t)}{S_{sat}^{FP}}+\frac{N_p\beta\tau_{21}\tau_p^{EC}I_{inj}}{e\tau_{sp}(1+\frac{\tau_{21}}{\tau_{31}})S_{sat}^{EC}}\right)S^{EC}(t)-\frac{\left(S^{EC}(t)\right)^2}{S_{sat}^{EC}}}{1+\frac{S^{FP}(t)}{S_{sat}^{FP}}+\frac{S^{EC}(t)}{S_{sat}^{EC}}}$$

(16)

In the interval $I_{th}^{EC}\langle I_{inj}\langle I_{th}^{FP}$ (i.e., $1\langle b\langle 1.4545$), corresponding to a current below the FP threshold, only the EC mode S^{EC} is present and corresponds to a stable state. Then, Eq. (16) reduce to a first order differential equation. By applying the method of partial fraction and integrating for both sides, Eq. (16) becomes

$$\int\left(\frac{\alpha}{CS^{EC}(t)+B+\sqrt{B^2-4AC}}+\frac{\beta}{CS^{EC}(t)+B-\sqrt{B^2-4AC}}\right)dS^{EC}(t) = \int\frac{dt}{\tau_p^{EC}\rho_{cav}}, \quad (17)$$

Where the coefficients *A*, *B*, *C*, α, and β are defined as

$$A = \frac{N_p\beta\tau_p^{EC}\tau_3 I_{inj}}{\tau_{sp}e},$$

$$B = \frac{1}{2}\left(\frac{I_{inj}}{I_{th}^{EC}}-1+\frac{N_p\beta\tau_{21}\tau_p^{EC}I_{inj}}{\tau_{sp}e(1+\frac{\tau_{21}}{\tau_{31}})S_{sat}^{EC}}\right),$$

$$C = -1/S_{sat}^{EC},$$

$$\alpha = \frac{-C}{2}-\frac{C-MB}{2\sqrt{B^2-4AC}},$$

$$\beta = \frac{-C}{2}+\frac{C-MB}{2\sqrt{B^2-4AC}}, \quad (18)$$

Now, we derive the times t_d^{EC}, Δt_{rise}^{EC}, and t_{ss}^{EC} using Eq.(17).

Derivation of the delay time: The delay time t_d^{EC} is the time elapses between the moment the bias is applied and the time the EC photon number reaches 10% of its stationary value. To derive t_d^{EC} we apply Eq.(17) and integrating it from 0 to 10%

value S^{EC} for number of photons, and from zero to t_d^{EC} for time. *i.e.*,

$$\int_0^{0.1S^{EC}} \left(\frac{\alpha}{CS^{EC}(t)+B+\sqrt{B^2-4AC}} + \frac{\beta}{CS^{EC}(t)+B-\sqrt{B^2-4AC}} \right) dS^{EC}(t) = \int_0^{t_d^{EC}} \frac{dt}{\rho_{cav}\tau_p^{EC}} . \tag{19}$$

The integration gives us

$$t_d^{EC} = \frac{\rho_{cav}\tau_p^{EC}}{\frac{I_{inj}}{I_{th}^{EC}}-1} \left(\ln\left(1+\frac{1}{10}\frac{\tau_{sp}\eta_r}{\beta\tau_3}\frac{I_{th}^{EC}}{I_{inj}}\left(\frac{I_{inj}}{I_{th}^{EC}}-1\right)^2 \right) - \frac{I_{inj}}{I_{th}^{EC}} \ln\left(\frac{9}{10}\right) \right) . \tag{20}$$

Derivation of the rise time: Now, to compute the rise time Δt_{rise}^{EC}, *i.e.,* the time taken for S^{EC} to rise from 10% to 90% of its stationary value, we use the Eq.(17) and integrating it from 10% to 90% value S^{EC} for number of photons , and from zero to Δt_{rise}^{EC} for time. *i.e.*,

$$\int_{0.1S^{EC}}^{0.9S^{EC}} \left(\frac{\alpha}{CS^{EC}(t)+B+\sqrt{B^2-4AC}} + \frac{\beta}{CS^{EC}(t)+B-\sqrt{B^2-4AC}} \right) dS^{EC}(t) = \int_0^{\Delta t_{rise}^{EC}} \frac{dt}{\rho_{cav}\tau_p^{EC}} . \tag{21}$$

The integration gives us after some algebra

$$\Delta t_{rise}^{EC} = \left(\frac{I_{inj}/I_{th}^{EC}+1}{I_{inj}/I_{th}^{EC}-1} \right) \rho_{cav}\tau_p^{EC} \ln 9 . \tag{22}$$

Derivation of the TSSE: The TSSE (t_{ss}^{EC}), *i.e.*, the time that elapses between the moment the bias is applied and the time the EC photon number reaches its stationary value, we use the Eq.(17) and integrating it from zero to steady-state value S^{EC} for number of photons, and from zero to t_{ss}^{EC} for time. *i.e.*,

$$\int_0^{S^{EC}} \left(\frac{\alpha}{CS^{EC}(t)+B+\sqrt{B^2-4AC}} + \frac{\beta}{CS^{EC}(t)+B-\sqrt{B^2-4AC}} \right) dS^{EC}(t) = \int_0^{t_{ss}^{EC}} \frac{dt}{\rho_{cav}\tau_p^{EC}} . \tag{23}$$

Finally, the steady-state under the effect of external cavity occurs approximately at the time

$$t_{ss}^{EC} = \frac{\rho_{cav}\tau_p^{EC}}{\left(\frac{I_{inj}}{I_{th}^{EC}}-1\right)} \left(\ln\left(\frac{I_{inj}}{I_{th}^{EC}}-1\right) - \frac{I_{inj}}{I_{th}^{EC}} \ln\left(\frac{\beta\tau_{21}S_{sat}^{EC}}{\tau_{sp}\eta_r\left(1+\frac{\tau_{21}}{\tau_{31}}\right)} \frac{I_{inj}}{I_{th}^{EC}} \right) + \frac{1}{2}\left(\frac{I_{inj}}{I_{th}^{EC}}+1\right) \ln S_{sat}^{EC} \right. +$$

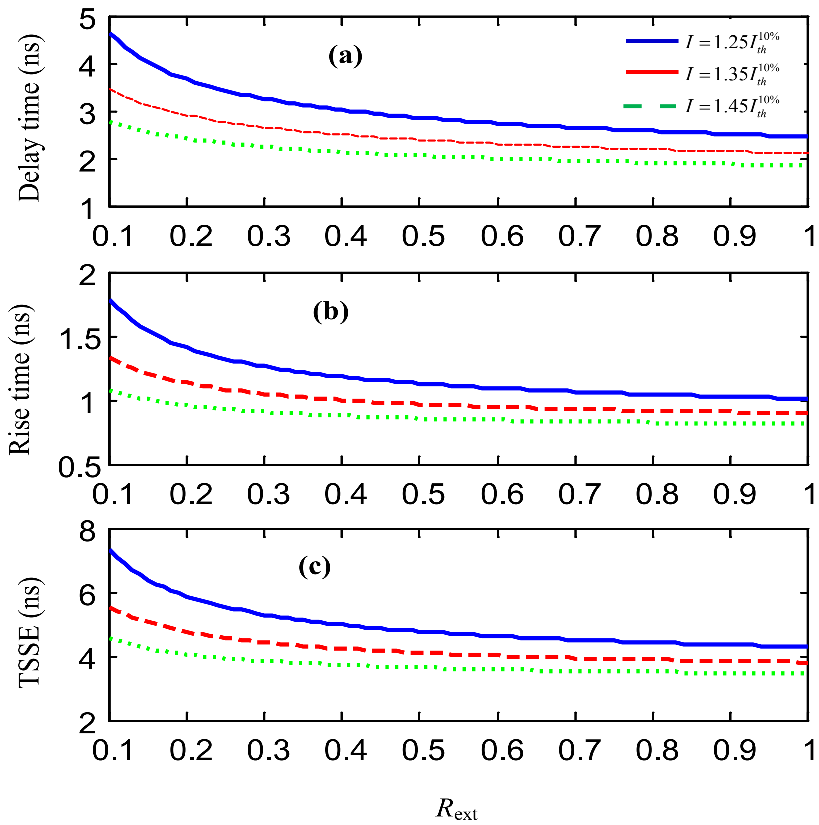

Figure 5: Effect of external cavity reflectivity (R_{ext}) on delay time t_d^{EC}, rise time Δt_{rise}^{EC} and TSSE t_{ss}^{EC} for three current injection. Blue solid line ($I_{inj} = 1.25 I_{th}^{10\%}$), red dashed line ($I_{inj} = 1.35 I_{th}^{10\%}$), and green dotted one ($I_{inj} = 1.45 I_{th}^{10\%}$). The external cavity length is $L_{ext} = 8$ cm.

$$+\rho_{cav}\tau_p^{EC}\left(1+\frac{\tau_{21}}{\tau_{31}}\right)\frac{\eta_r\tau_{sp}}{\beta\tau_{21}}\ln\left(\frac{\beta\tau_{21}^2}{\tau_{sp}\tau_3\eta_r\left(1+\frac{\tau_{21}}{\tau_{31}}\right)^2}+1\right). \quad (24)$$

We shows in Figure 5a, Figure 5b and Figure 5c the variation of the (a) delay time t_d^{EC}, (b) rise time Δt_{rise}^{EC}, and (c) TSSE t_{ss}^{EC} of the EC-QC laser as a function of the external cavity reflectivity which we vary from 10% to 100%. The results are all obtained for three values of the injection current below external cavity threshold. It is worthwhile to stress the strong decrease of t_d^{EC}, Δt_{rise}^{EC}, and t_{ss}^{EC} as the external reflectivity R_{ext} increases from its minimal value upward. This decrease are due to the strong dependence of the threshold current I_{th}^{EC} on photon lifetime τ_p^{EC}, where τ_p^{EC} is strongly affected by the external reflectivity value. We also see that the times t_d^{EC}, Δt_{rise}^{EC}, and t_{ss}^{EC} decrease with increasing current injection. The physical reason of this result is apparent: High external cavity reflectivity leads to low external cavity threshold values, thereby increasing the ratio of bias to threshold current. Finally, the different times are of the order of few nanoseconds.

We conclude our analysis with Figure 6a, Figure 6b, and Figure 6c, where we show the variation of the delay time t_d^{EC}, (b) rise time Δt_{rise}^{EC}, and (c) TSSE t_{ss}^{EC} of the EC-QC laser as a function of the external cavity length L_{ext} which we vary from 1 to 12 cm. The results are all obtained for three values of the injection current below EC threshold. We can immediately see that the times t_d^{EC}, Δt_{rise}^{EC}, and t_{ss}^{EC}, starting respectively from 0.5 ns, 0.25 ns, and 1 ns at $L_{ext}=1$ cm, increase with the external cavity length and depend strongly on current injection at high L_{ext}. The times t_d^{EC} and Δt_{rise}^{EC}, increase significantly when the current injection is reduced, and these lead to an important increases of the TSSE t_{ss}^{EC}.

Conclusion

Using a simple rate equations model, we developed an analytical scheme to derive the dynamical characteristics such as delay time, rise time, and TSSE as functions of current injection and the external cavity parameters of the system of a QC laser. We find as excepted that the threshold current decreases from 0.275 A at R_{ext} = 10% to 0.195 A for R_{ext} = 100%. Our numerical results also show that the current injection and the external cavity parameters affect the dynamical characteristics quite strongly.

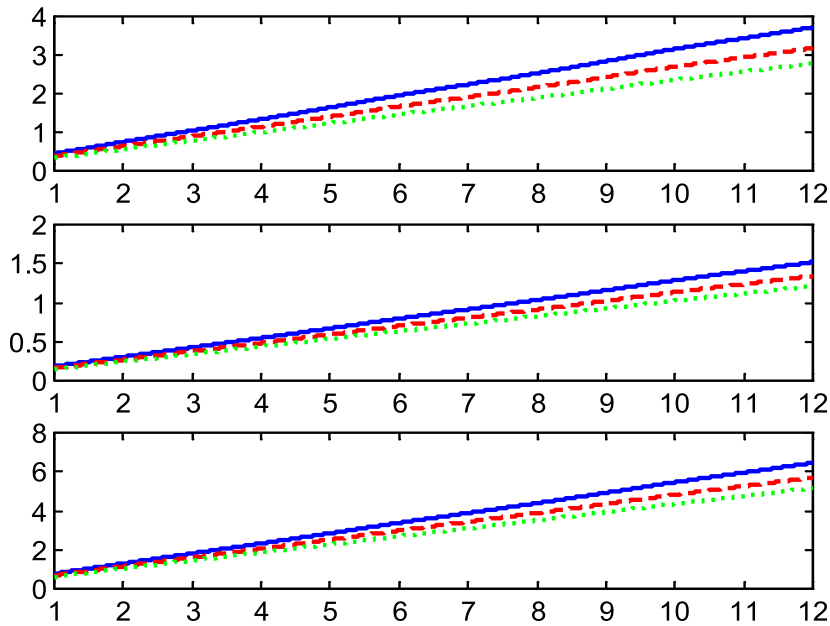

Figure 6: Effect of external cavity length (L_{ext}) on delay time t_d^{EC}, rise time Δt_{rise}^{EC} and TSSE t_{ss}^{EC} for three current injection. Blue solid line ($I_{inj}=1.25I_{th}^{10\%}$), red dashed line ($I_{inj}=1.35I_{th}^{10\%}$), and green dotted one ($I_{inj}=1.45I_{th}^{10\%}$). The external cavity reflectivity is R_{ext} = 90%.

Acknowledgments

The author is grateful to the Algerian Ministry of Higher Education for a research grant.

References

1. Faist J, Capasso F, Sivco DL, Sirtori C, Hutchinson AL, Cho AY (1994) Quantum cascade laser. Science 264: 553-556.
2. Luo GP, Peng C, Le HQ, Pei SS, Hwang WY, et al. (2001) Grating-tuned external-cavity quantum-cascade semiconductor lasers. Appl Phys Lett 78: 2834-2836.
3. Luo GP, Peng C, Le HQ, Pei SS, Lee H, et al. (2002) Broadly wavelength-tunable external cavity, mid-infrared quantum cascade lasers. IEEE J Quantum Electron 38: 486-494.
4. Totschnig G, Winter F, Pustogov V, Faist J, Muller A (2002) Mid-infrared external cavity quantum-cascade laser. Opt Lett 27: 1788-1790.
5. Peng C, Luo GP, Le HQ (2003) Broadband, continuous, and fine-tune properties of external-cavity thermoelectric-stabilized mid-infrared quantum-cascade lasers. App Opt 42: 4877-4882.
6. Peng C, Zhang HL, Le HQ (2003) Mid-infrared external-cavity two-segment quantum cascade laser. App Phys Lett 83: 4098-4100.
7. Maulini R, Beck M, Faist J, Gini E (2004) Broadband tuning of external cavity bound-to-continuum quantum-cascade lasers. Appl Phys Lett 84: 1659-1661.
8. Maulini R, Yarekha DA, Bulliard JM, Giovannini M, Faist J (2005) Continuous wave operation of a broadly tunable thermoelectrically cooled external cavity quantum cascade laser. Opt Lett 30: 2584-2586.
9. Maulini R, Mohan A, Giovannini M, Faist J, Gini E (2006) External cavity quantum-cascade laser tunable from 8.2 to 10.4 μm using a gain element with a heterogeneous cascade. Appl Phys Lett 88: 201113.
10. Wysocki G, Lewicki R, Curl RF, Tittel FK, Diehl L, et al. (2008) Widely tunable mode-hop free external cavity quantum cascade lasers for high resolution spectroscopy and chemical sensing. Appl Phys B 92: 305-311.
11. Maulini R, Dunayevskiy I, Lyakh A, Tsekoun A, Patel C, et al. (2009) Widely tunable high-power external cavity quantum cascade laser operating in continuous-wave at room temperature. Electron Lett 45: 107-108.
12. Hinkov B, Yang Q, Fuchs F, Bronner W, Kohler K, et al. (2009) Time-resolved characterization of external-cavity quantum-cascade lasers. App Phys Lett 94: 221105.
13. Hugi A, Maulini R, Faist J (2010) External cavity quantum cascade laser. Semicond Sci Technol 25: 083001.
14. Yang QK, Hinkov B, Fuchs F, Bronner W, Köhler K, et al. (2010) Rate equations analysis of external-cavity quantum cascade lasers. J Appl Phys 107: 043109.
15. Hamadou A (2018) The effect of external cavity reflectivity on the dynamic behaviors of quantum cascade laser. Chines J Phys 56: 1286-1295.
16. Iotti RC, Rossi F (2005) Microscopic theory of semiconductor-based optoelectronic devices. Rep Prog Phys 68: 2533-2571.
17. Yamanishi M, Edamura T, Fujita K, Akikusa N, Kan H (2008) Theory of the intrinsic line width of quantum cascade lasers: hidden reason for the narrow linewidth and line-broadening by thermal photons. IEEE J Quantum Electron 44: 12-29.
18. Maulini R (2009) Broadly tunable mid-infrared quantum cascade lasers for spectroscopic applications. VDM Verlag, Saarbrücken, Germany.
19. Olsson A, Tang CL (1981) Coherent optical interference effects in external-cavity semiconductor lasers. IEEE J Quantum Electron 17: 1320-1323.
20. Hamadou A (2015) Analytical investigation of the dynamics behaviors of quantum cascade laser. Optics commun 335: 271-278.

ISSN 2631-5092

9 772631 509009

DOI: 10.35840/2631-5092/4520